Glaucoma

Macular Ganglion Cell–Inner Plexiform Layer: Automated Detection and Thickness Reproducibility with Spectral Domain–Optical Coherence Tomography in Glaucoma

Jean-Claude Mwanza,[1] *Jonathan D. Oakley,*[2] *Donald L. Budenz,*[1] *Robert T. Chang,*[1,3] *O'Rese J. Knight,*[1,4] *and William J. Feuer*[1]

Purpose. To demonstrate the capability of SD-OCT to measure macular retinal ganglion cell–inner plexiform layer (GCIPL) thickness and to assess its reproducibility in glaucomatous eyes.

Methods. Fifty-one glaucomatous eyes (26 mild, 11 moderate, 14 severe) of 51 patients underwent macular scanning using the Cirrus HD-OCT (Carl Zeiss Meditec, Dublin, CA) macula 200×200 acquisition protocol. Five scans were obtained on 5 days within 2 months. The ganglion cell analysis (GCA) algorithm was used to detect the macular GCIPL and to measure the thickness of the overall average, minimum, superotemporal, superior, superonasal, inferonasal, inferior, and inferotemporal GCIPL. The reproducibility of the measurements was evaluated with intraclass correlation coefficients (ICCs), coefficients of variation (COVs), and test-retest standard deviations (TRTSDs).

Results. Segmentation and measurement of GCIPL thickness were successful in 50 of 51 subjects. All ICCs ranged between 0.94 and 0.98, but ICCs for average and superior GCIPL parameters (0.97–0.98) were slightly higher than for inferior GCIPL parameters (0.94–0.97). All COVs were <5%, with 1.8% for average GCIPL and COVs for superior GCIPL parameters (2.2%–3.0%) slightly lower than those for inferior GCIPL parameters (2.5%–3.6%). The TRTSD was lowest for average GCIPL (1.16 μm) and varied from 1.43 to 2.15 μm for sectoral GCIPL

Conclusions. The Cirrus HD-OCT GCA algorithm can successfully segment macular GCIPL and measure GCIPL thickness with excellent intervisit reproducibility. Longitudinal monitoring of GCIPL thickness may be possible with Cirrus HD-OCT for assessing glaucoma progression. (*Invest Ophthalmol Vis Sci.* 2011;52:8323–8329) DOI:10.1167/iovs.11-7962

Although glaucoma is classified as an optic nerve disease, pathologically it is characterized by the death of retinal ganglion cells (RGCs) and their axons. Traditionally, loss of RGCs has been judged based on damage to the optic nerve head (ONH) and visual field (VF) deficits. Because these assessments do not exactly reflect the extent to which the RGC population is affected, it became evident that any method enabling measurement of RGCs would advance both early detection and longitudinal monitoring of glaucoma. Advances in ocular imaging techniques, particularly the advent of optical coherence tomography (OCT), have enabled assessment of RGC axons by measuring the thickness of the peripapillary retinal nerve fiber layer (RNFL). In addition to peripapillary RNFL, OCT devices can measure the thickness of the whole retina, particularly in the macular area. Decreases in macular thickness that are believed to be due to loss of RGCs and that correlate with both RNFL thickness and VF defects have been reported in glaucomatous eyes.[1–8] However, measuring the whole macular thickness as a surrogate for glaucoma has the disadvantage of taking into account cell layers (i.e., outer retinal layers) that are not affected in glaucoma, thus obscuring the actual contribution of the RGC layer to the process.

Since its introduction, OCT has undergone several improvements, the latest of which is spectral domain (SD) technology. More recent advances in segmentation algorithms by several research groups have made possible the visualization and measurement of individual retinal layers with OCT in the macular region.[6,9–18] Anatomically, the human retina contains more than 1 million RGCs, with substantial interindividual variability; approximately 50% of the cells are concentrated within 4.5 mm of the fovea.[19] Although there is no variability in the RGC population in this small parafoveal area, there is, in contrast, considerable variability in the entire retina, resulting in variability in the number of axons in the peripapillary region.[19]

Glaucoma preferentially affects the ganglion cell complex (GCC), which is the sum of the three innermost layers: the RNFL, which is composed of axons; the ganglion cell layer (GCL), which is composed of cell bodies; and the inner plexiform layer (IPL), which contains the RGC dendrites. A few recent studies[20–22] have shown that measurement of macular GCC thickness has the same glaucoma diagnostic performance as RNFL thickness. However, it is possible that including the RNFL in the measurement may affect the diagnostic ability of GCC thickness. An underlying assumption here is that the ganglion cell structure differs less in a normal population than do other diagnostically important structures such as the RNFL

From the [1]Bascom Palmer Eye Institute, Miller School of Medicine, University of Miami, Miami, Florida; and [2]Voxeleron, LLC, Pleasanton, California.

Present affiliations: [3]Department of Ophthalmology, Stanford University, Palo Alto, California; and [4]Department of Ophthalmology, Case Western University, Cleveland, Ohio.

Presented in part at the annual meeting of the Association for Research in Vision and Ophthalmology, Fort Lauderdale, Florida, May 2011.

Supported by National Institutes of Health Grant P30 EY014801, an unrestricted grant from the Research to Prevent Blindness, and research support from Carl Zeiss Meditec, Inc.

Submitted for publication May 30, 2011; revised July 28 and September 4, 2011; accepted September 8, 2011.

Disclosure: **J.-C. Mwanza**, Carl Zeiss Meditec (F); **J.D. Oakley**, Carl Zeiss Meditec (E); **D.L. Budenz**, Carl Zeiss Meditec (F); **R.T. Chang**, Carl Zeiss Meditec (F); **O.J. Knight**, Carl Zeiss Meditec (F); **W.J. Feuer**, Carl Zeiss Meditec (F)

Corresponding author: Donald L. Budenz, Bascom Palmer Eye Institute, 900 NW 17th Street, Miami, FL 33136; dbudenz@med.miami.edu.

and the ONH. As such, the potential sensitivity of a measurement that is compared with that in a normal population could be higher because the difference would more likely be the result of pathologic change than of normal variation. This is a working hypothesis because until the advent of SD-OCT, we have been unable to study this in a reliable way. Furthermore, it is also hypothesized that the normal ganglion cell structure has symmetries that could be exploited in attempting to detect loss; an example would be a temporal defect in the anatomy corresponding to a nasal step in the VF. Including the RNFL in the measurement would make exploiting such symmetries in the analyses impossible.

The purpose of this study was to demonstrate the capability of the ganglion cell analysis (GCA) developed for Cirrus HD-OCT (Carl Zeiss Meditec, Dublin, CA) to automatically segment macular layers, to measure the thickness of the complex ganglion cell–inner plexiform layer, referred to in this study as GCIPL, and to assess its intervisit reproducibility.

Patients and Methods

Patients

The study protocol was approved by the Institutional Review Board of the University of Miami Miller School of Medicine and was conducted in accordance with the tenets of the Declaration of Helsinki. Subjects were 51 volunteers with glaucoma who were between 46 and 87 years of age (mean age, 70.9 ± 11.2 years) and had various degrees of disease severity based on the mean deviation grouping of the Hodapp-Parrish-Anderson scale.[23] Inclusion criteria were best-corrected visual acuity of ≥20/40 in the study eye and no history or evidence of retinal (diabetic retinopathy, macular degeneration, retinal detachment, epiretinal membrane) or nonglaucomatous optic nerve diseases, treatment that might be toxic to the retina or optic nerve (e.g., chloroquine, ethambutol), laser therapy, or ocular surgery within 1 month of enrollment. Each patient had a definite diagnosis of glaucoma based on glaucomatous damage to the optic disc and abnormal VF with or without elevated IOP. At least two VF analyzer (Humphrey; Carl Zeiss Meditec, Inc.) tests using the SITA standard 24–2 program were required, with the most recent within 12 months of enrollment. VFs were abnormal at the time of diagnosis if any of the following was true: glaucoma hemifield test result reliably outside normal limits; pattern standard deviation (PSD) $P < 5\%$; cluster of three or more points in the PSD plot in the superior or inferior hemifield with $P < 5\%$, including one or more with $P < 1\%$. Only one eye was randomly selected per patient.

Optical Coherence Tomography Image Acquisition and Processing

Three-dimensional cube OCT data were obtained from eyes dilated with tropicamide 1% and phenylephrine 2.5% with the same Cirrus HD-OCT device using the Macular Cube 200×200 scan protocol and processed with a prototype algorithm (prerelease version) that is intended to be incorporated into the Cirrus 6.0 software. This protocol performs 200 horizontal B-scans comprising 200 A-scan per B-scan over 1024 samplings within a cube measuring 6 × 6 × 2 mm (Fig. 1A) and is designed for retinal topography analysis. Five scans per eye obtained on 5 days within 2 months were used to calculate the intervisit measurement variability. Images with signal strength <6 (per manufacturer recommendation) and those with visible eye motion or blinking artifacts were considered of poor quality and discarded.

The GCA algorithm identifies the outer boundary of the RNFL (using a different method than in the peripapillary scans) and the outer boundary of the IPL. The difference between the RNFL and the IPL outer boundary segmentations yields the combined thickness of the RGC layer and the IPL. In the image data, the boundary between these two layers is anatomically indistinct so that they are difficult to distinguish from each other, but the combined thickness is considered to be indicative of the health of RGCs. The average, minimum (lowest GCIPL thickness over a single meridian crossing the annulus), and sectoral (superotemporal, superior, superonasal, inferonasal, inferior, inferotemporal) thicknesses of the GCIPL are measured in an elliptical annulus (dimensions: vertical inner and outer radius of 0.5 mm and 2.0 mm, horizontal inner and outer radius of 0.6 and 2.4 mm, respectively) around the fovea (Fig. 1A). The size and shape of the annulus are the result of a preliminary analysis performed using GCIPL maps of 47 healthy eyes. The size of the inner ring was chosen to exclude the area where the GCL is thin and difficult to detect, whereas the dimension of the outer ring was selected to conform closely to the real anatomy of the macular region, where the GCL is thickest in a normal eye. Data were processed with a prototype algorithm that is intended to be incorporated into the Cirrus 6.0 software. The algorithm processes data from either of the 3D volume scans from Cirrus; both scan patterns cover the same physical field of view, namely 6 × 6 × 2 mm,

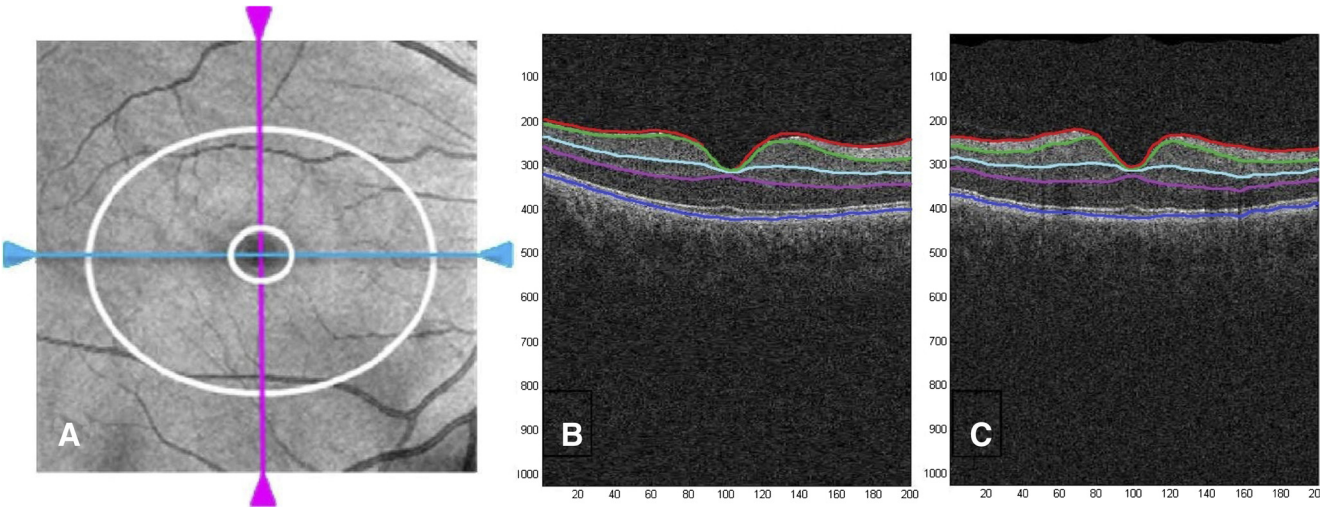

Figure 1. Cirrus OCT en face image (**A**) displaying the 6 × 6 mm portion of the retina scanned by the acquisition protocol with the annulus (area between the two white rings) within the cube used by the Cirrus GCA algorithm to measure the thickness of the GCIPL. (**B**, **C**) Segmentation of macular intraretinal layers from a horizontal and a vertical tomogram, respectively, with the Cirrus GCA algorithm. Boundaries (*top to bottom*): *red*, internal limiting membrane; *green*, RNFL-RGC boundary; *light blue*, IPL-INL boundary; *magenta*, IPL-OPL boundary; *dark blue*, Bruch's membrane. Layers (*top to bottom*): RNFL, GCIPL, internal nuclear layer (INL), and OPL/photoreceptors.

but the image data dimensionality is either 512 × 128 × 1024 or 200 × 200 × 1024. The input image data are initially segmented using the existing Cirrus inner limiting membrane (ILM) and RPE segmentation algorithms to create a region of interest within which lie the intraretinal layers. The algorithm continues in such a hierarchical approach, segmenting first the outer boundary of the outer plexiform layer (OPL), followed by the outer boundary of the IPL, and last the outer boundary of the RNFL. The segmentation procedure operates entirely in three dimensions and uses a graph-based algorithm to identify each layer. Image data are transformed into cost images such that the graph algorithm can find the lowest cost surface. To do this, the input data are initially median filtered to reduce speckle noise. They then create cost images based on directional edge-filtered images that have been enhanced to highlight specific boundary intensity changes using a sigmoid function. These are combined with positional cost images to form a single representation that is partitioned by the graph segmentation algorithm. The segmentation that results is globally optimal in terms of its cumulative cost for each of the layers.

The software analyzes the values, compares them to the device's internal normative database, and generates a thickness map, a deviation map, and a significance map color-coded to match RNFL thickness, with values within the normal range in green (P = 5%–95%), borderline values in yellow (1% < P < 5%), and values outside the normal range in red (P < 1%). The normative database contains data from 282 healthy subjects (133 men, 149 women) aged 19 to 84 years (mean age, 48.2 ± 16.9 years). Ethnicity breakdown of the Cirrus RNFL and macula normative databases was as follows: 43% Caucasian, 24% Asian, 18% African American, 12% Hispanic, 1% Indian, and 6% mixed ethnicity. Mean values were as follows: axial length, 23.94 ± 1.06 mm (range, 20–28 mm); IOP, 14.0 ± 2.4 mm Hg (range, 8–20 mm Hg); refraction expressed as spherical equivalent, −0.9 ± 2.1 D (range, −10.6 to +6.25 D); central corneal thickness (CCT), 549.58 ± 36.67 μm (mean, 449–662 μm); and VF field mean deviation, 0.02 ± 1.04 dB (range, −2.07 to +2.58 dB). All ILM and RNFL scans and those posterior to the IPL and OPL boundaries were manually reviewed for accuracy. The segmentation result was overlaid onto the OCT volume data and visualized in computing software (MatLab; MathWorks, Natick, MA), which often allows visualizing algorithm errors in the en face thickness maps. Any scan with an apparent segmentation error detected during this process was excluded from the study. More specifically, each B-scan was reviewed to check that the segmentation error of the ILM, OPL, or inner segment/outer segment boundary was <10 pixels for >75% of all A-scans within the annulus region. Any scan that did not meet this criterion was excluded.

Statistical Analysis

The statistical significance of differences between VF severity groups was assessed with ANOVA and subsequent post hoc least significant difference tests as appropriate. The total variability of all measurements was partitioned into variance components because of differences between patients and between days within patients (test-retest). Reproducibility was assessed with intraclass correlation coefficient (ICC), coefficient of variation (COV), and pooled within-subject test-retest SD (TRTSD). The numerator of the between-visit COV was the intervisit TRTSD, the square root of the pooled within-patient test-retest variance component.

Results

Demographic Characteristics

A total of 51 glaucomatous eyes, including 26 with mild, 11 with moderate, and 14 with severe glaucoma, were studied. One patient with mild glaucoma was excluded from the final statistical analysis because of algorithm segmentation failure that resulted in erroneous measurements. Thus, only data from 50 patients were analyzed. Patients' ages ranged from 46 to 87 years (mean, 73.4 ± 11.4 years). Glaucoma severity groups did not differ with regard to age (73.60 ± 11.39 years for mild, 70.82 ± 11.78 years for moderate, and 75.21 ± 6.81 years for severe glaucoma; P = 0.64), but they significantly differed from each other with regard to VF mean deviation (−2.96 ± 1.41 dB, −8.84 ± 1.22 dB, and −18.01 ± 6.94 dB, respectively; P < 0.001).

Segmentation of Macular Layers, Measurement, and Reproducibility of GCIPL Thickness

Although for all parameters studied the mean thickness was observed to decrease from mild to moderate and from moderate to severe, none of these differences were statistically significant except for minimum and inferotemporal thickness (Table 1). The automated Cirrus HD-OCT GCA algorithm successfully segmented the macula (Figs. 1B, 1C) and measured the thickness of the GCIPL in all 50 patients. The output of the GCA analysis provides a GCIPL thickness map that has a central circular black area expressing the lack of RGCs in the fovea. In a normal eye (Fig. 2A), the central black area is surrounded by an orange and yellow ring, where orange indicates thicker GICPL than yellow. In glaucoma (Fig. 2B), RGC loss and, thus, GCIPL thinning is expressed by the fading of red and yellow and the appearance of more light blue areas as the disease progresses. Other than the thickness map, the analysis output also provides a deviation map (Fig. 2C) and a significance map (Fig. 2D).

Intervisit means, TRTSDs, COVs, and ICCs of GCIPL thickness parameters are given in Table 2. All ICCs ranged between 0.94 and 0.98, but ICCs for average GCIPL and superior parameters (range, 0.96–0.98) were slightly higher than for inferior parameters (range, 0.94–0.97). All COVs were <5%, with 1.8% for average GCIPL and COVs for superior parameters (range, 2.2%–3.0%) slightly lower than those of inferior parameters (range, 2.5%–3.6%). The high reproducibility of the GCIPL thickness is illustrated in Figure 3. The TRTSD was lowest for average GCIPL (1.16) and varied from 1.43 (superior sector) to 2.15 (inferior sector). Figure 4 plots the test-retest standard deviations versus the means of average GCIPL thickness for each of the 50 eyes in the study, showing no relationship between test-retest variability and thickness. For purposes of comparison, the reproducibility statistics for RNFL measurements in the same group of patients appear at the bottom of Table 2 and are similar to those of GCCIPL except for the nasal quadrant.

With regard to structure-function relationship, VF mean deviation significantly correlated with GCIL thickness of the superotemporal sector (r = 0.45; P = 0.001), minimum thick-

Table 1. Mean (SD) of GCIPL Thickness Parameters in Mild, Moderate, and Severe Glaucoma

GCIP Parameters	Mean (SD)			One-way ANOVA P
	Mild	Moderate	Severe	
Average	68.5 (8.2)	62.3 (4.9)	56.0 (5.2)	0.156
Minimum	61.0 (9.5)	52.1 (5.9)	48.9 (4.2)	0.031*
Superotemporal	68.7 (8.0)	63.2 (5.5)	54.6 (6.4)	0.06
Superior	72.3 (11.5)	64.0 (8.5)	57.5 (6.3)	0.266
Superonasal	73.9 (9.6)	68.7 (9.9)	59.7 (8.1)	0.601
Inferonasal	68.4 (9.2)	61.9 (7.6)	55.9 (5.9)	0.485
Inferior	63.3 (9.4)	58.3 (8.5)	54.3 (5.2)	0.504
Inferotemporal	63.6 (8.4)	57.4 (8.5)	53.3 (4.9)	0.030†

* Post hoc least significant difference tests demonstrated that the mild group was different from the severe group (P = 0.012).

† Post hoc least significant difference tests demonstrated that the mild group was different from the severe group (P = 0.017); the post hoc difference between mild and moderate was 0.059.

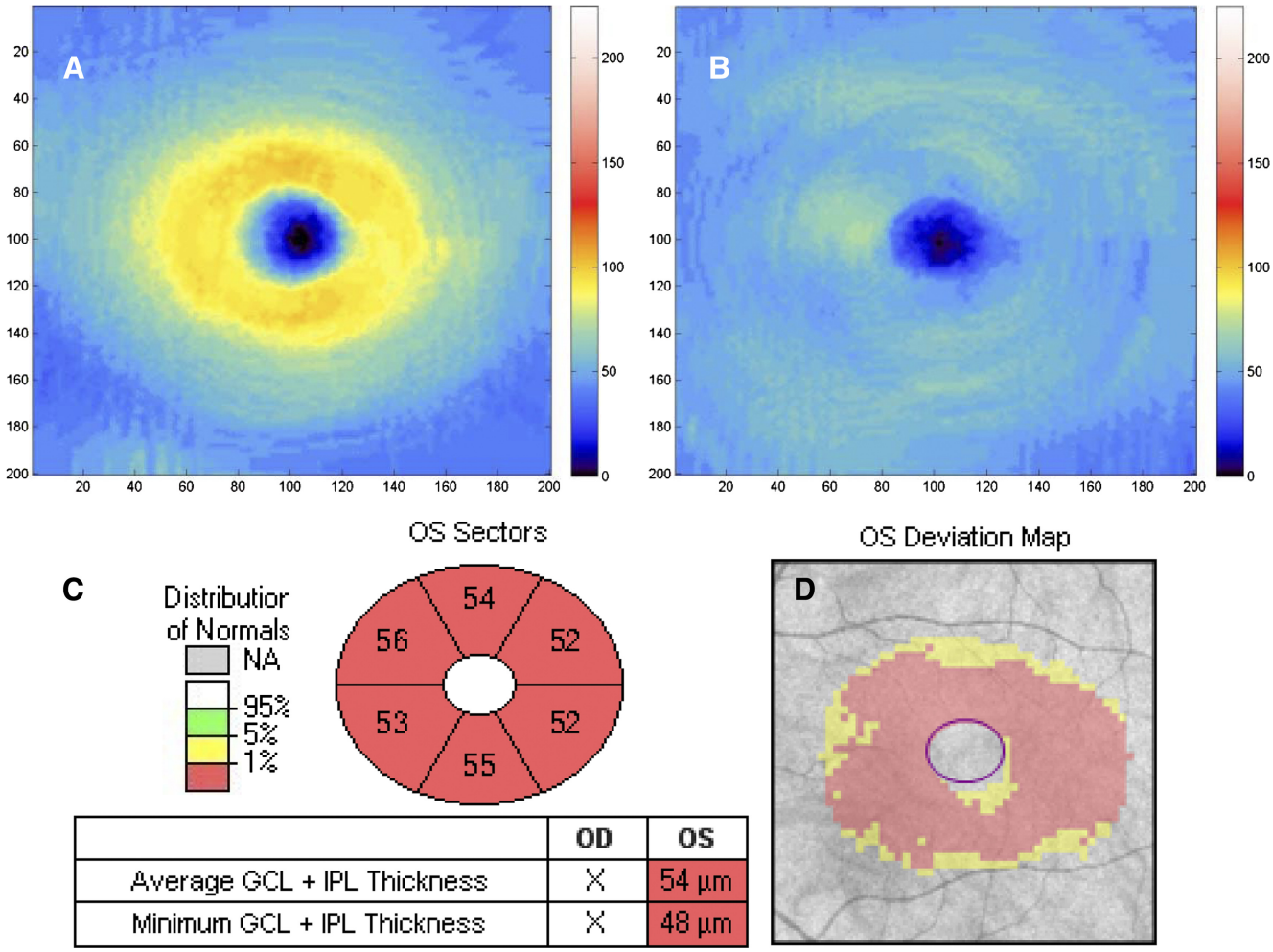

Figure 2. GCIPL thickness maps (the denser the orange/yellow ring, the thicker the GCIPL) of a normal eye (**A**) and an eye with severe glaucoma (**B**). GCIPL deviation map (**C**) and significance map (**D**) of the same eye shown in **B**. The *red* on the deviation map indicates regions with GCIPL thickness outside normal limits. The significance map shows (clockwise) thicknesses of the superior, superonasal, inferonasal, inferior, inferotemporal, and superotemporal sectors of the annulus and the average and minimum GCIPL (*box*).

ness of the GCIPL ($r = 0.39$; $P = 0.0.05$), GCIPL thickness of the inferotemporal sector ($r = 0.39$; $P = 0.005$), and average GCIPL ($r = 0.36$, $P = 0.011$) (Fig. 5). GCIPL thickness measurements in the superior, inferior, superonasal, and inferonasal sectors of the annulus did not significantly correlate with retinal sensitivity ($P > 0.05$).

Table 2. Intervisit Means, TRTSD, COV, and ICC of GCIPL and RNFL Thickness Parameters

Parameters	Mean	TRTSD (µm)	COV (%)	ICC (%)
Average GCIPL	62.9	1.16	1.8	0.98
Minimum GCIPL	54.8	2.28	4.2	0.94
Superotemporal GCIPL	62.8	1.87	3.0	0.96
Superior GCIPL	65.2	1.43	2.2	0.98
Superonasal GCIPL	67.9	1.80	2.7	0.97
Inferonasal GCIPL	62.8	1.93	3.1	0.96
Inferior GCIPL	59.1	2.15	3.6	0.94
Inferotemporal GCIPL	58.6	1.48	2.5	0.97
Average RNFL	62.5	1.64	2.6	0.97
Temporal RNFL	46.6	2.89	6.2	0.93
Inferior RNFL	69.4	2.91	4.2	0.97
Superior RNFL	75.4	2.95	3.9	0.97
Nasal RNFL	58.5	3.60	6.2	0.82

Discussion

Several potentially blinding eye diseases, such as age-related macular degeneration and glaucoma, cause structural changes in the retina and the choroid. Successful quantitative evaluation of these changes requires a segmentation-based determination of the thicknesses of tissue layers. Thickness measurements of macular layers with OCT rely on the development of robust and accurate algorithms for the segmentation of intraretinal layers. This is a time-consuming, difficult, and costly process that includes a lot of calculations, verifications, and validations, which may explain the limited availability of these algorithms on most commercially available OCT devices. For glaucoma patients, one of the most important layers that could be identified is the RGC. Thus, it is of paramount importance that imaging devices used for detecting glaucoma-related structural changes in the retina be able to identify this layer and measure its thickness. The results of the present study indicate that the Cirrus GCA segmentation algorithm allows identification of macular intraretinal layers and measurement of GCIPL thickness parameters with excellent reproducibility. Although further studies are necessary, these results suggest that this new algorithm has the potential to be useful for objective quantification of RGC damage in glaucoma.

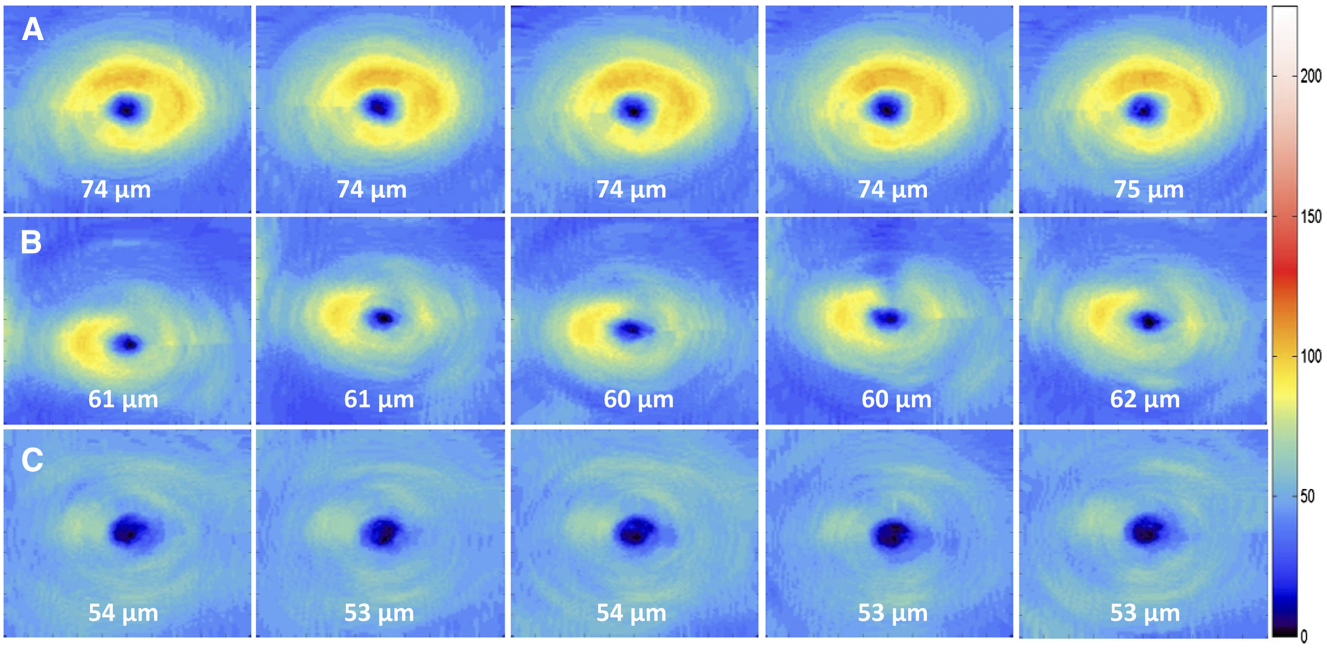

FIGURE 3. Intervisit reproducibility of GCIPL thickness measured from five different visits within a 2-month period for an eye with mild (**A**), moderate (**B**), and severe (**C**) glaucoma. Note the consistency in average GCIPL thickness over the five sessions in all three eyes.

One of the fundamental differences between traditional macular thickness and the macular GCIPL thickness measurements is the shape of the annulus used to measure them. While macular thickness is measured in an area whose circular shape is arbitrary and whose size (6-mm diameter) was chosen to cover the entire macular region,[24] the size and shape of the macular area used for GCIPL thickness measurements have an anatomic basis, as demonstrated by histology[19] and imaging (Knighton R, unpublished data, 2009).

Although in vivo quantitative evaluation of RGC axon health through RNFL thickness measurement with OCT has rapidly become part of the diagnosis and long-term monitoring of glaucoma, such an approach for RGC bodies has been recently introduced for clinical use. It has long been suggested that glaucoma-induced structural changes may start in the macula because of the dense population of RGCs in this region. This assumption is supported by experimental models of glaucoma that showed substantial loss of RGCs in the parafoveal region.[25,26] To date, there are few reports on measurements of RGC layer thickness in glaucoma using OCT. However, most of them have focused on the GCC.[13,20,22,27] Additionally, there is increasing interest in assessing how RGC layer thickness measurement with OCT may help in the diagnosis and follow-up of glaucoma. Wang et al.[6] were among the first to report on the feasibility of measuring the thickness of the RGC layer in glaucomatous eyes with an SD-OCT device (3D-OCT 1000; Topcon Corporation, Tokyo, Japan). However, their segmentation was performed manually rather than automatically. Manual segmentation is laborious and time consuming and may be subject to intraobserver and interobserver variability. OCT retinal image analysis software (OCTRIMA) developed by DeBuc et al.[9] and used with Stratus OCT was also shown to be capable of detecting and measuring intraretinal layers, including the GCIP, in normal eyes. Compared with algorithms used by Wang et al.[6] and DeBuc et al.,[9] the Cirrus HD-OCT GCA algorithm has the advantage of segmenting the layers automatically and rendering the measurements of eight different parameters rather than only the average GCIPL. This facilitates objective comparison and helps choose the best parameter. Another segmentation algorithm, developed by Bagci et al.,[28] detected seven intraretinal boundaries and allowed determination of the thickness profile of six retinal layers, including the GCIPL, using both Stratus OCT and Fourier domain OCT (RTVue-100; Optovue, Freemont, CA) in 15 and 10 normal eyes, respectively. Measurements obtained along 6 mm with Stratus OCT and 5 mm with Fourier domain OCT (RTVue-100; Optovue) around the fovea were similar (68 ± 23 μm for automated segmentation and 69 ± 22 μm for manual segmentation). These values were lower than ours, probably because the macular area in which the measurements were taken was larger, thus containing areas in which the GCIPL is thinner. Chiu et al.[29] also recently tested an algorithm that accurately segmented the GCIPL and seven other retinal layers in normal eyes using a Bioptigen SD-OCT system (Bioptigen Inc., Research Triangle Park, NC), with good agreement between observers and between manual and automatic segmentations.

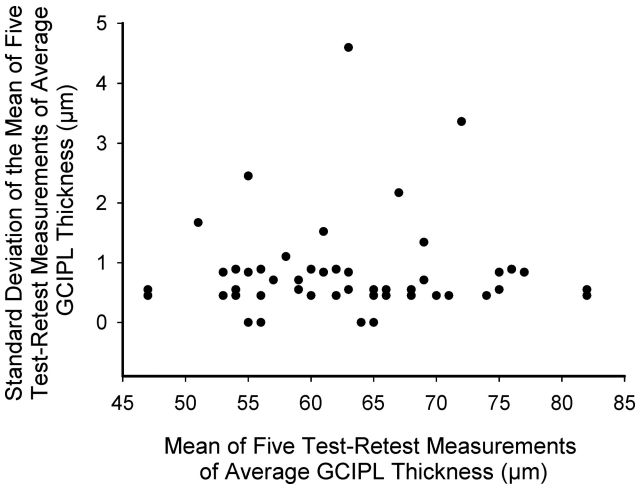

FIGURE 4. Scatter plot of the relationship between the test-retest standard deviations versus the mean of average GCIPL thickness for each of the 50 eyes in the study.

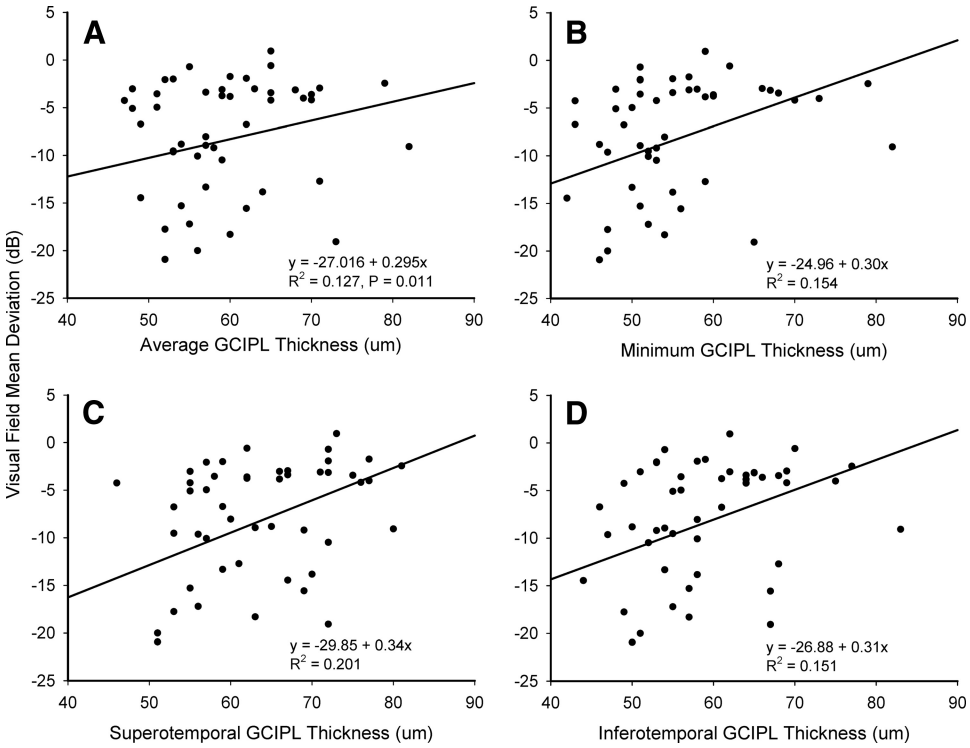

FIGURE 5. Linear regression plot of the relationship between VF mean deviation and average GCIPL thickness (**A**), minimum GCIPL thickness (**B**), and GCIPL thickness of the superotemporal (**C**) and inferotemporal (**D**) sectors of the macular.

As with any new technique, the reproducibility of GCIPL thickness measurements obtained with the Cirrus HD-OCT GCA algorithm is of prime clinical importance if it is to be used for glaucoma detection and its longitudinal monitoring for change. From the technical standpoint, the high reproducibility found in this study was due to automatic detection and registration of the center of the macula using the algorithm included in the Cirrus software before placing the analysis annulus (Durbin et al. Improved repeatability using postacquisition registration and fovea finding on images from Cirrus HD-OCT. ISIE 2009, oral communication). Although measured in strikingly different patient groups, our ICC for average GCIPL is similar to that reported by DeBuc et al.[9] using Stratus OCT in normal eyes. However, their intervisit COV and TRTSD were higher than in the present study. The reproducibility of morphometric measurements is driven by several factors, one of which is image resolution. Thus, the discrepancy in COV and TRTSD is likely due to the difference in image resolution between Stratus OCT and Cirrus OCT devices. Because of the limitations associated with ICC, particularly when making comparisons outside the population analyzed, we presented three assessments of reproducibility: the ICC, COV (which is, of course, also limited by the population studied), and the TRTSD. This last statistic was calculated with a variance component analysis, which is a form of mixed model. This measure is not scaled to the population analyzed and so is more robust. In fact, all methods of assessing test-retest reproducibility may be misleading if generalized to populations other than the ones analyzed. This is true of all inferential statistics and is the reason we sought to include measurements made on glaucoma patients with a wide range of disease severity. Overall, the results herein presented showed excellent intervisit reproducibility of all eight parameters in glaucomatous eyes, making the GCIPL thickness an additional attractive potential marker for disease detection and progression. Although previous studies have reported similar glaucoma diagnostic ability for GCC and RNFL thickness measurements,[20,22,27] further investigation will be needed to determine how the GCIPL performs compared with both GCC and RNFL thickness. Moving forward, it is hoped that the available SD-OCT instruments equipped with a broadband light source can provide improved contrast and resolution of outer retinal layers and capabilities to separate the GCL and the IPL for better evaluation of changes to individual layers in glaucoma.

In conclusion, a novel SD-OCT algorithm for segmenting retinal layers, with emphasis on the GCIPL, is proposed. This algorithm shows great potential for quantitative analysis of retinal layer thickness. Its ability to quantify the GCIPL with excellent intervisit reproducibility may improve the diagnosis, staging, and monitoring of glaucoma.

References

1. Giovannini A, Amato G, Mariotti C. The macular thickness and volume in glaucoma: an analysis in normal and glaucomatous eyes using OCT. *Acta Ophthalmol Scand Suppl.* 2002;236:34–36.
2. Greenfield DS, Bagga H, Knighton RW. Macular thickness changes in glaucomatous optic neuropathy detected using optical coherence tomography. *Arch Ophthalmol.* 2003;121:41–46.
3. Guedes V, Schuman JS, Hertzmark E, et al. Optical coherence tomography measurement of macular and nerve fiber layer thickness in normal and glaucomatous human eyes. *Ophthalmology.* 2003;110:177–189.
4. Kanadani FN, Hood DC, Grippo TM, et al. Structural and functional assessment of the macular region in patients with glaucoma. *Br J Ophthalmol.* 2006;90:1393–1397.
5. Takagi ST, Kita Y, Takeyama A, et al. Macular retinal ganglion cell complex thickness and its relationship to the optic nerve head topography in glaucomatous eyes with hemifield defects. *J Ophthalmol.* 2011;2011:914250.
6. Wang M, Hood DC, Cho JS, et al. Measurement of local retinal ganglion cell layer thickness in patients with glaucoma using frequency-domain optical coherence tomography. *Arch Ophthalmol.* 2009;127:875–881.
7. Wollstein G, Schuman JS, Price LL, et al. Optical coherence tomography (OCT) macular and peripapillary retinal nerve fiber layer measurements and automated visual fields. *Am J Ophthalmol.* 2004;138:218–225.

8. Zeimer R, Asrani S, Zou S, et al. Quantitative detection of glaucomatous damage at the posterior pole by retinal thickness mapping: a pilot study. *Ophthalmology.* 1998;105:224–231.
9. DeBuc DC, Somfai GM, Ranganathan S, et al. Reliability and reproducibility of macular segmentation using a custom-built optical coherence tomography retinal image analysis software. *J Biomed Opt.* 2009;14:064023.
10. Fabritius T, Makita S, Miura M, et al. Automated segmentation of the macula by optical coherence tomography. *Opt Express.* 2009; 17:15659–15669.
11. Garvin MK, Abramoff MD, Kardon R, et al. Intraretinal layer segmentation of macular optical coherence tomography images using optimal 3-D graph search. *IEEE Trans Med Imaging.* 2008;27: 1495–1505.
12. Garvin MK, Abramoff MD, Wu X, et al. Automated 3-D intraretinal layer segmentation of macular spectral-domain optical coherence tomography images. *IEEE Trans Med Imaging.* 2009;28:1436–1447.
13. Ishikawa H, Stein DM, Wollstein G, et al. Macular segmentation with optical coherence tomography. *Invest Ophthalmol Vis Sci.* 2005;46:2012–2017.
14. Kajic V, Povazay B, Hermann B, et al. Robust segmentation of intraretinal layers in the normal human fovea using a novel statistical model based on texture and shape analysis. *Opt Express.* 2010;18:14730–14744.
15. Mishra A, Wong A, Bizheva K, et al. Intra-retinal layer segmentation in optical coherence tomography images. *Opt Express.* 2009;17: 23719–23728.
16. Quellec G, Lee K, Dolejsi M, et al. Three-dimensional analysis of retinal layer texture identification of fluid-filled regions in SD-OCT of the macula. *IEEE Trans Med Imaging.* 2010;29:1321–1330.
17. Rossant F, Ghorbel I, Bloch I, et al. Automated segmentation of retinal layers in OCT imaging and derived ophthalmic measures. *IEEE Trans Med Imaging.* 2009;28:1370–1373.
18. Yazdanpanah A, Hamarneh G, Smith B, et al. Intra-retinal layer segmentation in optical coherence tomography using an active contour approach. *Med Image Comput Comput Assist Interv.* 2009;12:649–656.
19. Curcio CA, Allen KA. Topography of ganglion cells in human retina. *J Comp Neurol.* 1990;300:5–25.
20. Kim NR, Lee ES, Seong GJ, et al. Structure-function relationship and diagnostic value of macular ganglion cell complex measurement using Fourier-domain OCT in glaucoma. *Invest Ophthalmol Vis Sci.* 2010;51:4646–4651.
21. Seong M, Sung KR, Choi EH, et al. Macular and peripapillary retinal nerve fiber layer measurements by spectral domain optical coherence tomography in normal-tension glaucoma. *Invest Ophthalmol Vis Sci.* 2010;51:1446–1452.
22. Tan O, Chopra V, Lu AT, et al. Detection of macular ganglion cell loss in glaucoma by Fourier-domain optical coherence tomography. *Ophthalmology.* 2009;116:2305–2314.
23. Hodapp E, Parrish RKI, Anderson DR. *Clinical Decisions in Glaucoma*. St. Louis: Mosby-Year Book; 1993.
24. Klein R, Davis MD, Magli YL, et al. The Wisconsin age-related maculopathy grading system. *Ophthalmology.* 1991;98:1128–1134.
25. Desatnik H, Quigley HA, Glovinsky Y. Study of central retinal ganglion cell loss in experimental glaucoma in monkey eyes. *J Glaucoma.* 1996;5:46–53.
26. Frishman LJ, Shen FF, Du L, et al. The scotopic electroretinogram of macaque after retinal ganglion cell loss from experimental glaucoma. *Invest Ophthalmol Vis Sci.* 1996;37:125–141.
27. Tan O, Li G, Lu AT, et al. Mapping of macular substructures with optical coherence tomography for glaucoma diagnosis. *Ophthalmology.* 2008;115:949–956.
28. Bagci AM, Shahidi M, Ansari R, et al. Thickness profiles of retinal layers by optical coherence tomography image segmentation. *Am J Ophthalmol.* 2008;146:679–687.
29. Chiu SJ, Li XT, Nicholas P, et al. Automatic segmentation of seven retinal layers in SDOCT images congruent with expert manual segmentation. *Opt Express.* 2010;18:19413–19428.